FACILE PREPARATION OF NANOSCALE α-Al_2O_3 VIA SUCROSE SOFT TEMPLATING

Received: 21-05-2025

Vu Thi Tan [*], La The Vinh, Quach Thi Phuong, Nguyen Hoang Tuan

School of Chemistry and Life Sciences, Hanoi University of Science and Technology, 1, Dai Co Viet, Hai Ba Trung, 10000, Ha Noi, Viet Nam

**Email: tan.vuthi@hust.edu.vn*

TÓM TẮT

NGHIÊN CỨU, CHẾ TẠO NANO α-Al_2O_3 BẰNG PHƯƠNG PHÁP KHUÔN MỀM SỬ DỤNG ĐƯỜNG SUCROSE

Trong nghiên cứu này các hạt α-Al_2O_3 kích thước nano đã được tổng hợp bằng phản ứng nhiệt sinh sử dụng đường sucrose vừa làm tác nhân khử (nhiên liệu), vừa làm khuôn mềm. Sản phẩm α-Al_2O_3 thu được đã được phân tích bằng các kỹ thuật SEM, XRD và DLS. Kết quả XRD xác nhận sự hình thành các tinh thể nano α-Al_2O_3, trong khi ảnh SEM cho thấy kích thước hạt nằm trong phạm vi kích thước nano. Nghiên cứu cho thấy việc tăng nồng độ đường sucrose dẫn đến sự hình thành các hạt α-Al_2O_3 nhỏ hơn. Kết quả chỉ ra khi tang nồng độ sucrose trong dung dịch thì kích thước hạt α-Al_2O_3 sẽ trở nên nhỏ hơn, với đường kính trung bình dưới 50 nm. Công trình này giới thiệu việc ứng dụng mới của sucrose trong quy trình chế tạo bột α-Al_2O_3 kích thước nano. Nghiên cứu mở ra hướng mới trong việc sản xuất các hạt nano oxit nhôm pha α ổn định, có tiềm năng ứng dụng trong nhiều lĩnh vực khác nhau.

***Từ khoá*:** *Khuôn mềm, phương pháp đốt cháy; hạt nano, α-Al_2O_3; đường*

1. INTRODUCTION

Alumina was one of the most widely used materials today, serving as a versatile material in many applications[1]. Due to its ample polymorphism, aluminum oxide exhibited multiple phases that influenced its surface properties and microstructure[2]. Recently, alumina had widely been used in many catalytic support applications due to its high porosity [3]. However, the refractory and heat-resistant properties of supporting material were required in some applications. Therefore, it was necessary to convert γ-phase into α-phase because of the low temperature resistance of γ-Al_2O_3. The α- Al_2O_3 was known as a material with thermodynamically stable, chemically inert, and excellent temperature resistant [4]. But, α- Al_2O_3 could be obtained only at about 1200º C, however at high temperatures alumina could be aggregated and making a large particle size and small surface area. This results making α-form was not suited for catalyst support and in grinding ball application [5].

Recently, several research groups have shown that nanocrystalline Al_2O_3 displayed a great toughness, hardness, thermal and chemical stability [6] [7]. However, the structural imperfection of this material could reduce these properties [8], [9], [10]. The high-purity, uniformly sized, equiaxed nanoparticles of Al_2O_3 might make it to be high performance nanoceramics. Rabindra et al. used thermal decomposition of Al-ion to produce α-Al_2O_3 nanocrystals (15–20 nm), with a BET surface area of 194 m^2/g

[11]. However, the high porosity of alumina might present several drawbacks in applications performed at high temperature.

At a recent time, various synthesizing α-alumina methods were studied, for example precipitation, combustion, microwave, wet chemical, and sol-gel techniques [12] [13] [14], [15], [16] [17],. The particle size obtained in those mentioned methods providing particles typically between 60–500 nm. For example, Hasanpoor et al. [15] obtained Al_2O_3 with the size of 200–300 nm using plant extracts. But the scalability in a large production was limited due to several drawbacks such as low yield, poor uniform in morphology. Additionally, combustion synthesis stood out for its simplicity and effectiveness, using aluminium nitrates and fuel in exothermic reactions reaching >1200°C [18]. Recent studies demonstrated that aluminum nitrate could produce α-Al_2O_3 nanoparticles sized in the range of 100 nm at 900–1100°C [17]. The way to produce α-Al_2O_3 with nanosize below 100 nm was still difficult at the present time.

This study introduced a novel, low-cost, and scalable method using distinct amount of sucrose as a fuel additive to produce pure nanocrystalline α-Al_2O_3 at 1200°C. The result might provide a scalable methodology for the fabrication of α-Al_2O_3 nanoparticles.

2. METHOD

2.1. Preparation method

Both materials $Al(NO_3)_3$ and sucrose (from Xilong) were used a precursor and fuel, respectively, to synthesize α-Al_2O_3 nanoparticle. Sucrose was gradually added to 50 ml solution of $Al(NO_3)_3$ at varying concentrations. The obtained mixture was constantly stirred for two hours to ensure its homogeneity. After that, the solution was evaporated to acquire a slurry mixture. Then, the obtained slurry was then roasted at 250º C for several hours, causing sucrose decomposition and the formation of black foam. The mixture was expanded 4-8 times during dehydration of sucrose to form a charcoal. Finally, the foam was treated at 1200º C for two hours in air to obtain α-Al_2O_3 nanoparticle powder.

2.2. Material characterization

The X-ray diffraction (XRD) patterns of samples were recorded using a Bruker D8 Advance apparatus at 40 kV and 40 mA, using Cu Kα radiation (λ = 0,15406 nm). The crystal size values were determined from the XRD pattern using Scherrer's equation (d_{XRD}). The morphology of the samples was studied using scanning electron microscopy (SEM, FEI Quanta FEG 650 model) DLS analysis is utilized in Malvern 2000. The elemental composition of the alumina was investigated using XRF spectroscopy (SRS 3000 Bruker) and LECO combustion analysis GDS900.

III. RESULT AND DISCUSSION

3.1. The influence of sucrose concentration on the yeild of Al_2O_3.

In order to study the effect of distinct amount sucrose, the $Al(NO_3)_3$ and sucrose molar ratio was varied in the range of 0.5-4 (Table 1).

Table 1: The $Al(NO_3)_3$ and sucrose ratio during the combustion reaction.

Sample denote	$Al(NO_3)_3$: sucrose (molar ratio)	Yeild,%
Al-1-0	1:0	93,7
Al-1-0,5	1:0,5	92,9
Al-1-1	1:1	94,5
Al-1-2	1:2	96,1
Al-1-4	1:4	93,8

The result presented in Table 1 demonstrates that sucrose did not affect to the yeild of Al_2O_3.

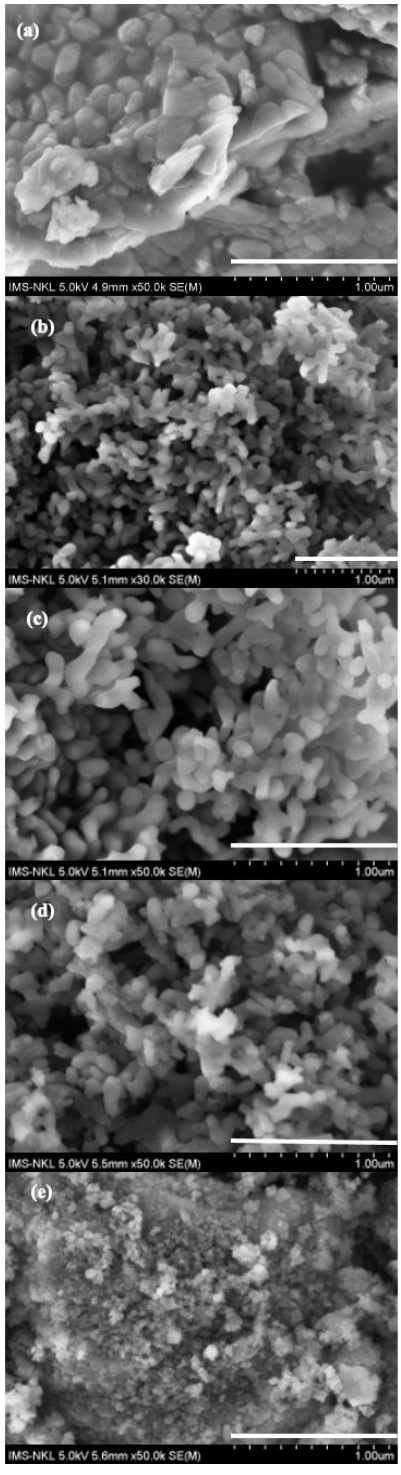

Figure 1: SEM images of (a) Al-1-0; (b)-Al-1-0,5; (c)-Al-1-1; (d)-Al-1-2; (e)-Al-1-4.

However, the main of this study aimed to investigate the effects of sucrose on the size of α- Al_2O_3 nanoparticles. Therefore, higher sucrose concentration is expected to reduce crystal size of alumina. We already knew that, $Al(NO_3)_3 \cdot 9H_2O$, with diameter of Al^{3+} cations was 0.53 nm, which was used as the alumina source. The purpose of this study was that sucrose coated the alumina cations to limit crystal growth of the formed alumina oxide. Thus, the produced product might present a small particle size which is suitable for catalyst and ball milling application.

3.2. Characterization of the prepared Al_2O_3

In this work, the microstructure and morphology of alumina oxide was analyzed using SEM technique. Figure 1a showed the agglomerated particle of Al_2O_3 with the absence of sucrose. The obtained material with sizes ranging from 300 to 700 nm. These particles formed bulk Al_2O_3. The Al_2O_3 particles from thermal degradation in the presence of sucrose as fuel were shown in Figures 1b,c and d,e. It could be seen that, using sucrose as fuel and template resulted in more homogeneous particle size and morphology (Figures 1d–e). Additionally, the particle size dramatically decreased with rising sucrose concentration.

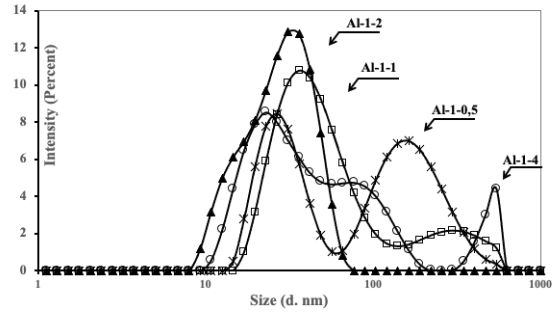

Figure 2: DLS results of Al-1-0,5; Al-1-1; Al-1-2; Al-1-4

Figure 2 showed the DLS particle size distribution of obtained Al_2O_3 samples.

DLS was vital technique for studying particle size and predicting agglomeration or size uniformity. However, this analysis technique might sometimes give false results because of self-agglomeration particles. Figure 2 showed that all samples in the presence of sucrose had Al_2O_3 particles smaller than 100 nm, except the sample Al-1-0.5, which provided particle size larger than 1000 nm. At the high sucrose concentration (Al-1-2), the particle sizes were in the range 20–50 nm. For the sample Al-1-4, two particle size ranges were presented: under 100 nm and also a small size around 1000 nm. This phenomenon was possibly due to carbon residue from sucrose during thermal calcination at 1200°C.

To evaluate the effect of sucrose on Al_2O_3 particle size during $Al(NO_3)_3$ decomposition, we compared DLS data from samples with and without sucrose.

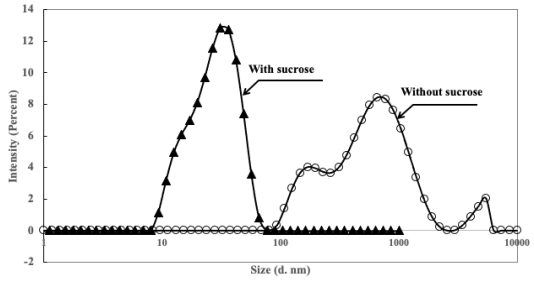

Figure 3: DLS results of sample with sucrose and without sucrose

Figure 3 showed that, after thermal calcination, the carbon from sucrose was absolutely burned off, making to the formation of Al_2O_3 nanoparticles. In the absent of sucrose, the obtained Al_2O_3 showed significantly sizeable particles, even larger than 1000 nm in size.

The SEM and DLS results showed that sucrose played an important role in the preventing self-agglomeration during thermal decomposition and resulting in nano-sized Al_2O_3 particles. The possibly mechanism could be described as $Al(NO_3)_3$ decomposes, sucrose gradually carbonizes into charcoal, which preventing agglomeration during the thermal decomposition at initial stage (200-250º C) [19].

To define the crystal phase of the obtained alumina, the X-ray diffraction (XRD) patterns was performed for all nano-sized Al_2O_3 samples (Figure 4). Diffraction peaks at 25.55, 35.13, 37.74, 43.35, 52.54, 57.46, 66.48, and 68.21 were observed, corresponding to Miller indices 012, 104, 110, 013, 024, 116, 214, and 300. These peaks were directly associated to the hexagonal phase of bulk Al_2O_3. The space group R3c, from JCPDS-ICDD file no. 46-1212, was used to define the diffraction peaks. Figure 4 presented only diffraction peaks of α-Al_2O, the absence of impurity diffraction peaks indicated that all powder samples illustrate high purity.

Table 2: FRX results of Al-1-0,5; Al-1-1; Al-1-2; Al-1-4 samples

Samples	Element	Mass %
Al-1-0,5	Al_2O_3	99.1
	MgO	0.05
	CuO	0.08
	ZnO	0.03
Al-1-1	Al_2O_3	99.2
	MgO	0.10
	CuO	0.12
	NiO	0.09
Al-1-2	Al_2O_3	99.4
	MgO	0.08
	CuO	0.06
	NiO	0.04
Al-1-4	Al_2O_3	98.3
	MgO	0.05
	NiO	0.06
	SiO_2	0.09

The elemental composition of obtained α-Al_2O_3 nanoparticles was analyzed using X-ray fluorescence (XRF) and LECO techniques. Recently, the FRX tool calculates chemical elements in the stable oxide form, which resulted in the total percentage of oxidized species exceeding 100%. In this work, the FRX data showed that the all samples provide nearly 100% α- Al_2O_3 (Table 2).

Table 3: LECO analysis of the obtained α-Al_2O_3 nanoparticles

Material	FRX analysis Al%	LECO analysis C%
Al-S-1-0,5	99.5	0
Al-S-1-1	99.4	0
Al-S-1-2	99.6	0
Al-S-1-4	98.5	0.59

The XRF analysis illustrated that all samples contained a small trace amount of other oxides, which due to the preparation step or impurities presented in precursors. Among these samples, Al-1-2 showed the highest purity form of α- Al_2O_3. LECO analysis was also used in this work to check for carbon impurity. The LECO result indicated that the sample with a lower sucrose concentration provided pure α- Al_2O_3, while the sample with higher sucrose amount had small trace carbon residue (Table 3). The excess carbon could affect the combustion of charred sucrose, and the formation of α-Al_2O_3 particles might have the carbon residue at 1200ºC.

At last, based on characterization results from SEM, DLS, XRD, LECO, and XRF analysis techniques, optimal synthesis condition of α-Al_2O_3 nanoparticles at 1200ºC required a ratio of sucrose and aluminum nitrate equal or less than 2.

4. CONCLUSIONS

In conclusion, the use of sucrose as fuel and template for the fabrication of α-Al_2O_3 nanoparticle offerred a straightforward method for producing stable α- alumina oxide in nanosize. To our knowledge, this was the first work of using sucrose as soft template and fuel combustion to generate stable α- Al_2O_3 nanoparticles. Analysis through SEM, XRD, and DLS revealed that the particle size ranges from 20 to 50 nm. XRD results further confirmed that the obtained particles were in the stable α- Al_2O_3 phase. This study presented a novel methodology for producing stable α-Al_2O_3 nanoparticles, with promising commercial application.

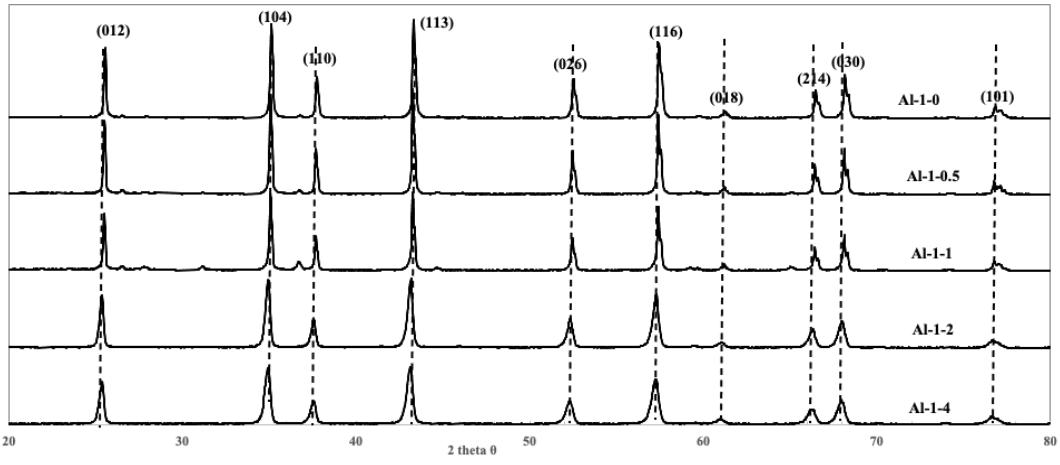

Figure 4: The X-ray diffraction (XRD) patterns of all nano-sized Al_2O_3 samples

Acknowledgements

The work was supported by Hanoi University of Science and Technology through the grant number T2023-PC-102.

REFERENCES

[1] Trueba M, Trasatti SP, (2005). γ-Alumina as a Support for Catalysts: A Review of Fundamental Aspects. *European Journal of Inorganic Chemistry*, **17**, 3393-3403.

[2]Kaunisto K, *(2023)*. Evolution of alumina phase structure in thermal plasma processing. *Ceramic International*, **13**, 21346-21354.

[3]Prins R, (2020). On the structure of γ-Al_2O_3, *Journal of. Catalysis*, **392**, 336-346.

[4]Suchanek WL, (2010). Hydrothermal Synthesis of Alpha Alumina (α-Al_2O_3) Powders: Study of the Processing Variables and Growth Mechanisms. *Journal of the American Ceramic Society* , **93**, 399-412.

[5] Shin H, Lee S, Suk Jung H, Kim JB, (2013). Effect of ball size and powder loading on the milling efficiency of a laboratory-scale wet ball mill. *Ceramic International*, **39**, 8963-8968

[6]Rice RW, Wu CC, Boichelt F, (2005). Hardness–Grain-Size Relations in Ceramic. *Journal of the American Ceramic Society*, **77**, 2539-2553.

[7]García Ferré F, (2024). The mechanical properties of a nanocrystalline Al_2O_3/a-Al_2O_3 composite coating measured by nanoindentation and Brillouin spectroscopy. *Acta Material*, **61**, 2662-2670.

[8] Kiennemann J, Pagnoux C, Chartier T, Baumard JF, and Lamérant JM, (2004). Influence of Impurities on Dispersion Properties of Bayer Alumina. *Journal of the American Ceramic Society*, **87**, 2175-2182.

[9]Das SR, Ghosh BP, Guha SK, (2025). Effect of Environmental Impurities on the Microstructure and Sinterability of Alumina Ceramics. *Transactions of the Indian Ceramic Society*, **45**, 152-155.

[10]Drahus MD, Chan HM, Rickman JM, Harmer MP, (2005). Densification and Grain Growth of Fe-Doped and Fe/Y Codoped Alumina: Effect of Fe Valency. *Journal of the American Ceramic Society*, 88, 3369-3373.

[11] Das RN, Bandyopadhyay A, Bose S, (2001). Nanocrystalline α-Al_2O_3 Using Sucrose. *Journal of the American Ceramic Society*, **84**, 2421-2423.

[12]Su X, Chen S, Zhou Z, (2012). Synthesis and characterization of monodisperse porous α-Al2O3 nanoparticles. *Applied Surface Science.*, **258**, 5712-5715.

[13] Prashanth PA, (2015). Synthesis, characterizations, antibacterial and photoluminescence studies of solution combustion-derived α-Al_2O_3 nanoparticles. J*ournal of the American Ceramic Society*, **3**, 345-351.

[14]Liu Q, (2021). Synthesis of thin alpha alumina platelets with a large aspect ratio. *Ceramic International*, **47**, 252-259.

[15] Hasanpoor M, Fakhr NH, Aliofkhazraei M, (2017). Microwave-Assisted Synthesis of Alumina Nanoparticles Using Some Plants Extracts. *Journal of Nanostructures*, **7**, 2017.

[16] Maleki B, Ashrafi SS, (2014). Nano α-Al_2O_3 supported ammonium dihydrogen phosphate ($NH_4H_2PO_4/Al_2O_3$): preparation, characterization and its application as a novel and heterogeneous catalyst for the one-pot synthesis of tetrahydrobenzo[b]pyran and pyrano[2,3-c]pyrazole derivatives. *RSC Advance*, **4**, 42873-42891.

[17]Suhanda RS, Frank E, (2021). Nanocrystalline α-Al_2O_3 powder preparation with sucrose as a template

through a chemical route. *Journal of Ceramic Processing Research*, **12**, 365-370.

[18] Parauha YR, Dhoble SJ, (2022). Rare-earth-activated phosphors for forensic applications. *Rare-Earth-Activated Phosphors*, **2022,** 215-246.

[19] Pacewska B, Keshr M, (2002). Thermal transformations of aluminium nitrate hydrate. *Thermochimica Acta*, **385**, 73-80.